Paper I

I

Narrow electrodes on YZ-$LiNbO_3$ as an alternative to etched grooves for dispersive delay lines

S. Härmä, C.-U. Kim,
S. M. Balashov, and V. P. Plessky

S. Härmä, C.-U. Kim, S. M. Balashov, and V. P. Plessky, "Narrow electrodes on YZ-$LiNbO_3$ as an alternative to etched grooves for dispersive delay lines", IEEE Transactions on Ultrasonics, Ferroelectrics, and Frequency Control, Vol. 55, No. 2, February 2008, pp. 494-498.

Correspondence

Narrow Electrodes on YZ-$LiNbO_3$ as an Alternative to Etched Grooves for Dispersive Delay Lines

Sanna Härmä, Che-Uk Kim, Sergei M. Balashov, and Victor P. Plessky, *Senior Member, IEEE*

***Abstract*—Narrow, open-circuited aluminum electrodes can provide controllable, weak reflectivity necessary for many applications such as surface acoustic wave (SAW) tags and dispersive delay lines (DDLs). We show, using finite- and boundary element method (FEM-BEM) based simulations and experiments, that a reflectivity of 0.3% per wavelength can be achieved easily and controlled by varying the electrode width.**

I. Introduction

Dispersive delay lines (DDLs) based on reflecting gratings, consisting of grooves on the surface of a substrate, were developed in the 1970s [1]. The operation of these devices relies on quasiperiodic reflectors with gradually changing and normally very weak reflectivity. In principle, this can be achieved by using either etched grooves or metal electrodes as reflecting elements. However, manufacturing grooves with their depth varying along the structure involves a complicated and time-consuming procedure demanding specialized technological equipment. In the days of intensive development of reflective array compressors (RACs) [1], electrodes were not a valid alternative to grooves: First, technological limitations forced the metal ratios to 0.5 at 500 MHz. Second, to achieve a wide band, strong piezoelectrics as substrate material are required. For such materials and electrode widths, the resulting reflectivities are a few percent per electrode and unacceptably high for most DDL applications. For these reasons, DDLs have remained very expensive and are produced on a piece-by-piece basis. At present, however, there is a renewed interest [2] to use them in such devices as ultra wide band (UWB) communication systems and real-time spectrum analyzers.

For a DDL having a center frequency f_c, band B, and dispersive delay time T, the number of reflectors efficiently reflecting the wave N_{eff} can be estimated as [3], [4]:

$$N_{\text{eff}} = \frac{f_c T}{\sqrt{BT}}. \tag{1}$$

Manuscript received June 19, 2007; accepted August 16, 2007.

S. Härmä and V. P. Plessky are with the Department of Engineering Physics, Helsinki University of Technology, FI-02015 TKK, Finland (e-mail: sanna.harma@tkk.fi).

V. P. Plessky also is with GVR Trade SA, Bevaix, Switzerland.

C.-U. Kim is with the University of Ulsan, Ulsan, South Korea.

S. M. Balashov is with EFTECH Co. Ltd., Cheongwon-gun, Cungbuk, South Korea.

Digital Object Identifier 10.1109/TUFFC.2008.667

Using the typical values $f_c = 400$ MHz, $B = 100$ MHz, and $T = 50$ μs ($BT = 5000$), gives $N_{\text{eff}} \approx 300$ for the number of reflectors operating more or less in phase at a given frequency. To avoid distortions of amplitude and phase, the device must work in the linear regime, i.e., the reflected amplitudes must be proportional to the reflector strengths, and have a low level of multiple reflections. This demands a small total reflectivity of the region effectively reflecting the waves, as we must have $rN_{\text{eff}} < 1$, where r is the reflectivity of a single electrode. For the typical, high-BT device described above, this condition becomes $r < 0.3\%$.

The characteristic wavelength in the above example is about 10 μm, and the electrode width for a metal ratio m/p of 0.5 is about 2.5 μm. However, modern standard photolithography allows for the manufacturing of 0.4-μm wide electrodes, which in our example corresponds to $m/p = 0.1$. This advance in technology allows us to replace the intricate and expensive etched grooves with much cheaper standard surface acoustic waves (SAW) technology involving only aluminum electrodes.

Reflectors with controllable reflectivity also are important for SAW tags [5], [6]. To achieve a reasonably high data capacity, a SAW tag must include about 50 reflecting electrodes. This implies that the reflectors in the beginning of the reflective array must have very weak reflectivities.

In this work, we show that reflectivities on the order of 0.3% per wavelength (per two electrodes) can be achieved for open aluminum electrodes with $m/p = 0.2$, and that such reflectivities can be controlled by varying the electrode width. We also demonstrate the use of narrow electrodes in an inline DDL.

II. Analysis of Simulated and Experimental Results

We study two types of test devices. The type 1 devices have two identical interdigital transducers (IDT) and a reflector placed in-between (Fig. 1). The type 2 structure consists of two tracks, each having two IDTs and a reflector at the end (Fig. 2). All devices are simulated using FEMSAW[1], a finite- and boundary element method (FEM-BEM) based software, and manufactured and probed on a YZ-$LiNbO_3$ wafer. The simulation results and experimental data for the type 1 devices are used to determine the reflectivity per wavelength $|\kappa\lambda_0|$ and the attenuation per wavelength $\gamma\lambda_0$ within the reflective arrays. The type 2 structure illustrates the principle of operation of an inline DDL using a special geometry for which the reflected signal can be directly seen in the S_{21} parameter of the device.

[1] http://www.gvrtrade.com

Fig. 1. Type 1 test structure. Two identical IDTs and a reflector in-between. Schematic drawing.

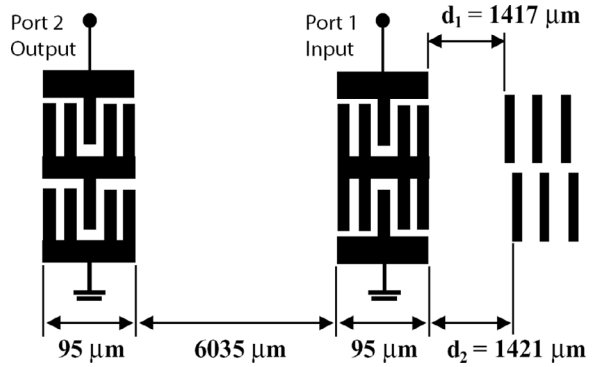

Fig. 2. Type 2 test structure. Two acoustic tracks, each having two IDTs and a reflector. Schematic drawing.

A. Geometry and Operation of Test Devices

The type 1 structure is a simplified version of the test bars used in [7] for characterization of SAW devices. It has two identical IDTs and a reflector, consisting of 49 open-circuited floating electrodes, placed halfway between the IDTs at a distance of 4.7 mm from each IDT. The IDTs have three electrodes per wavelength with the polarities hot-hot-ground and operate at $f_c = 201$ MHz. This IDT type was chosen for its lower reflectivity compared to a standard IDT. We study four structures that have different metal ratio in the reflectors varying from 0.2 to 0.5. Each structure has a variant for two metal thicknesses: $h/\lambda = 1.15\%$ and 1.73%. For type 1 devices, the reflectivity and attenuation parameters of the reflectors, $|\kappa\lambda_0|$ and $\gamma\lambda_0$, respectively, are extracted from the R/T ratio of the reflection and transmission coefficients.

The type 2 structure consists of two tracks. Each track has two IDTs and a reflector at the end. The reflectors are identical (38 electrodes, $m/p = 0.5$) but the distances d_1 and d_2 separating them from the input IDTs differ by $\lambda/4$. The relative metal thickness is 3.5%. The output IDTs are connected in series and in phase (the lower IDT is the exact copy of the upper one) and the input IDTs in series but in opposite phase (the lower IDT is identical to the upper one but flipped around the horizontal axis). Therefore, the direct signals generated by the input IDTs are cancelled when received by the output IDTs, which makes the two pairs of IDTs "mutually blind". Meanwhile, the signals that are generated by the input IDTs, reflected by the reflectors, and received by the output IDTs are summed in phase; they have opposite phases when generated, but their propagation paths differ by $\lambda/2$. For a type 2 device, the reflected signal thus can be directly seen in the S_{21} parameter. This idea can be used in inline DDLs in which it is important to create a signal without perturbation by any other strong signal.

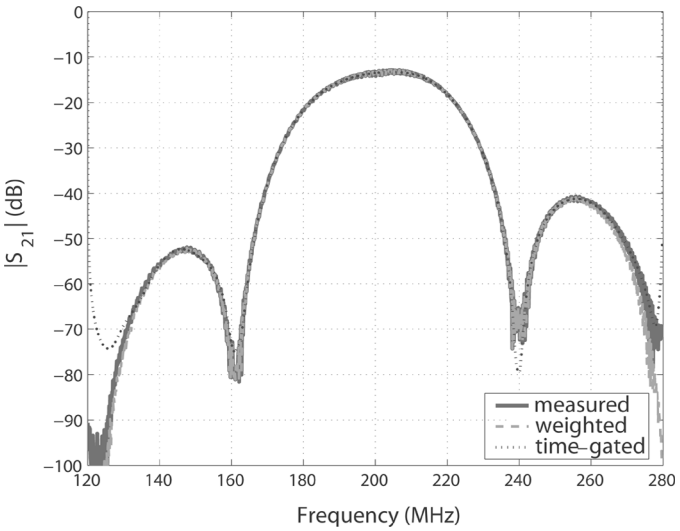

Fig. 3. $|S_{21}|$ in frequency domain for a type 1 device.

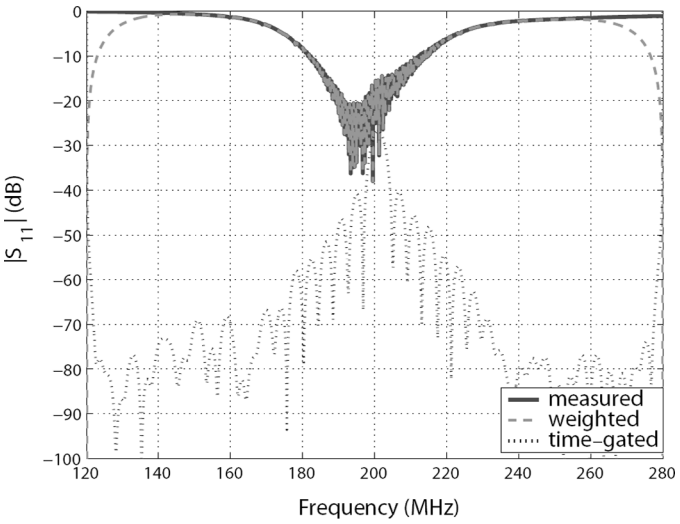

Fig. 4. $|S_{11}|$ in frequency domain for a type 1 device.

B. Processing of Data

For the type 1 devices, $|\kappa\lambda_0|$ and $\gamma\lambda_0$ are extracted using the R/T ratio, which is obtained in the following way (Figs. 3–6 illustrate the procedure). The S_{11} and S_{21} parameters are first weighted and Fourier transformed from frequency domain into time domain. Then the reflected signal (with the path input IDT-reflector-input IDT) is separated from the S_{11} data and the direct propagation signal (with the path input IDT-reflector-output IDT) from the S_{21} data. The time-gated data then are transformed back into frequency domain and used for calculating the R/T ratio. The IDT performance and the propagation loss have

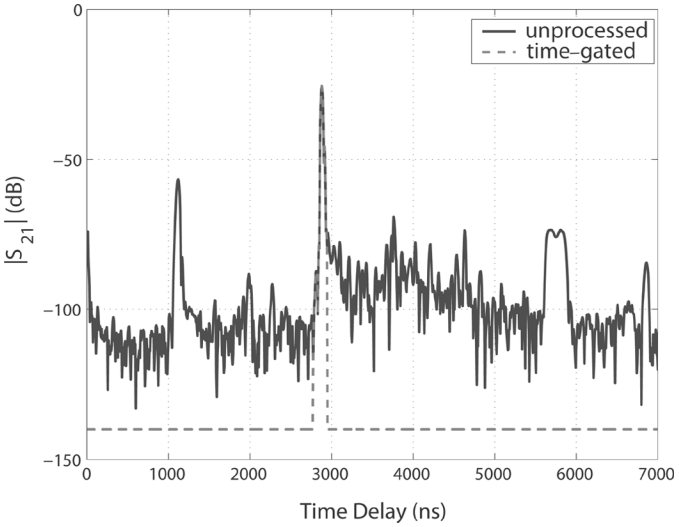

Fig. 5. $|S_{21}|$ in time domain for a type 1 device.

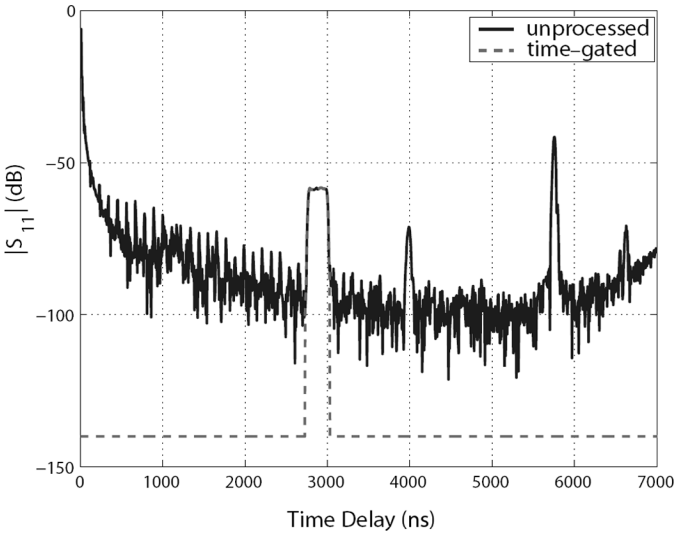

Fig. 6. $|S_{11}|$ in time domain for a type 1 device.

equal contributions in the time-gated S_{11} and S_{21} and are cancelled when the ratio S_{11}/S_{21} is calculated. Therefore, S_{11}/S_{21} of time-gated signals is in fact equivalent to the R/T of the reflector. The same procedure is used for both the simulated and the experimental results as well as for the type 2 devices. In their case, however, we are interested only in the S_{21} parameter, which is time-gated such that only the signal generated by the input IDT, reflected by the reflectors and received by the output IDT, is kept.

C. Extraction of Reflector Parameters

The reflector parameters $|\kappa\lambda_0|$ and $\gamma\lambda_0$ are determined using the $|R/T|$ curves of the type 1 devices. Fig. 7 shows this curve for one of the studied cases for both simulation and measurement. Reflectivity per wavelength $|\kappa\lambda_0|$ can be estimated as [8]:

$$|\kappa\lambda_0| = \frac{\lambda_0}{L}\,\mathrm{asinh}\left|\frac{R(f_c)}{T(f_c)}\right|, \tag{2}$$

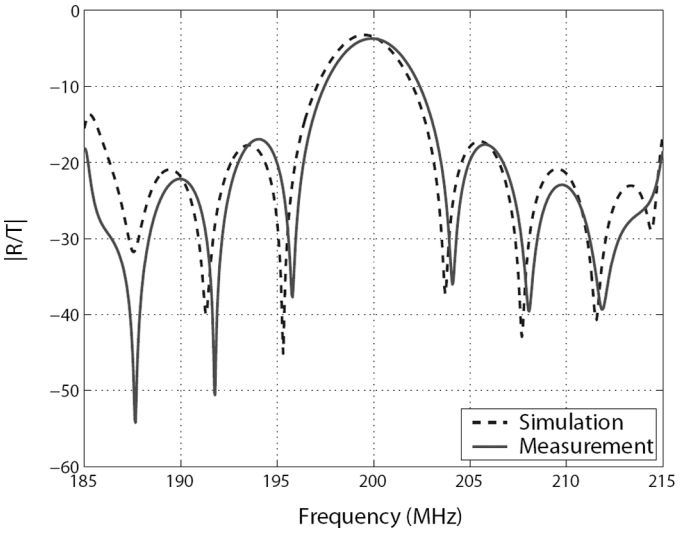

Fig. 7. Ratio $|R/T|$ for a type 1 test device.

TABLE I
MEASURED AND SIMULATED REFLECTIVITY AND ATTENUATION.

Metal thickness h/λ_0 (%)	Metal ratio m/p	Reflectivity $\|\kappa\lambda_0\|$ (%)		Attenuation $\gamma\lambda_0$ (10^{-3} Neper/λ_0)	
		Measured	Simulated	Measured	Simulated
1.15	0.2	0.33	0.55	4.39	0.44
1.15	0.3	0.83	1.17	3.36	0.58
1.15	0.4	1.55	1.98	1.49	1.15
1.15	0.5	N/A[1]	2.89	N/A	2.19
1.73	0.2	0.43	0.55	3.49	0.55
1.73	0.3	0.91	1.08	4.60	0.58
1.73	0.4	N/A	1.79	N/A	1.14
1.73	0.5	2.36	2.63	1.73	1.78

[1]NA = Not applicable.

where f_c is the center frequency, λ_0 is the wavelength of the reflector structure, and L is the reflector length ($L = N_{\mathrm{el}}p$, where N_{el} is the number of reflector electrodes and $p = \lambda_0/2$ is the pitch of the electrodes). The attenuation $\gamma\lambda_0$ (in Neper/λ_0) within the grating is given by:

$$\gamma\lambda_0 = \frac{4n^2\pi\left|\frac{R(f_{\pm n})}{T(f_{\pm n})}\right|}{\left|\frac{\Delta f_n}{f_c}\right|(N_{\mathrm{el}}-1)^3|\kappa\lambda_0|}, \tag{3}$$

which directly relates the notch depth to attenuation. In (3), f_n is the position of the n^{th} notch and:

$$\frac{\Delta f_n}{f_c} = \frac{f_n - f_{-n}}{f_n + f_{-n}}, \tag{4}$$

is the relative deviation from the center frequency of the grating [8]. In our case, $n = 1$ as we use the first notches around the center frequency.

The $|\kappa\lambda_0|$ and $\gamma\lambda_0$ extracted using (2) and (3) are summarized in Table I. For the narrowest electrodes ($m/p = 0.2$), reflectivities of 0.33% and 0.43% per λ_0 (per two electrodes) were achieved for the relative metal thicknesses of 1.15% and 1.73%, respectively. The values of attenuation

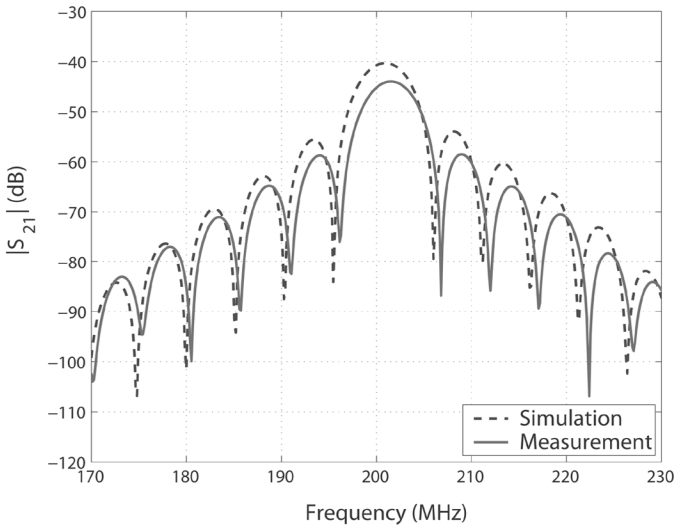

Fig. 8. $|S_{21}|$ for a type 2 test device.

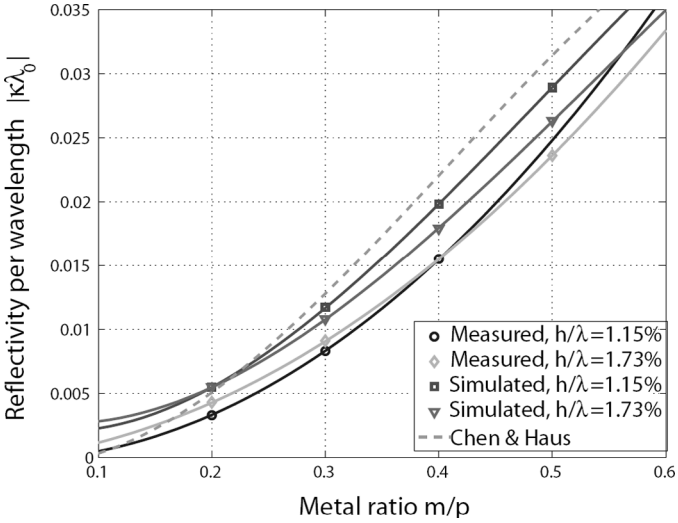

Fig. 9. Extracted reflectivities compared to the Chen and Haus data [9].

can be considered good estimates only because the notch depth is easily influenced by the finite frequency step, and especially for the narrowest electrodes, by electromagnetic (EM) feedthrough. Due to the symmetry of the device, an EM feedthrough signal and the reflected signal are received at the same time and are not separable using time gating. In simulations, we have used a slightly asymmetric structure to separate these two signals. In the experimental results, however, the signals are inseparable. Nevertheless, we believe that, for $m/p = 0.4$ and 0.5, attenuation is estimated correctly. In these cases, the obtained general level of attenuation is about $1 \cdot 10^{-3}$ to $2 \cdot 10^{-3}$ Neper/λ_0. For two devices, experimental data were quite uncertain and we prefer to present in Table I only the results of simulations. However, these cases involve only the widest electrodes with $m/p = 0.4$ and 0.5 and are not central to this paper.

Fig. 8 shows the absolute value of the S_{21} parameter, i.e., the reflected signal for a type 2 device. Contrary to type 1 devices, in which we use the R/T ratio, IDT losses are now present in the observed signal, and reflectivity cannot be directly extracted from the curves. Nevertheless, attenuation can be estimated using (2) and (3) and assuming that reflectivity per λ_0 is about 0.03. This yields an estimate of $3 \cdot 10^{-3}$ Neper/λ_0.

Fig. 8 also can be used for determining the SAW velocity within the grating. For the experimental case, we obtain $V_{\mathrm{SAW}} = f_c \lambda_0 \approx 3446.7$ m/s and for the theoretical case 3434.2 m/s. The distances between the notches are theoretically determined by the number of reflector electrodes. In our case, the predicted value is $f_0/N_{\mathrm{el}} \approx 5.2$ MHz; also the measurement data give 5.2 MHz and the simulation 5.1 MHz.

III. Discussion

Fig. 9 shows the extracted reflectivities as a function of metal ratio. It must be noted that the metal thicknesses are very small, only 1.15% and 1.73%. Therefore, reflectivity is mainly due to short-circuiting of the electric fields and not to mass loading. The experimental reflectivities are systematically a bit lower than those simulated, which can be an indication of over-etched electrodes. This hypothesis is supported by the fact that the relative discrepancy is smaller for wide electrodes, for which the over-etch would be relatively less important. The reason for the difference also can be too small loss parameters used in the simulations. For the narrowest electrodes ($m/p = 0.2$), we obtain experimentally $|\kappa\lambda_0| = 0.33\%$ and 0.43% (per two electrodes) for the relative metal thicknesses of 1.15% and 1.73%, respectively.

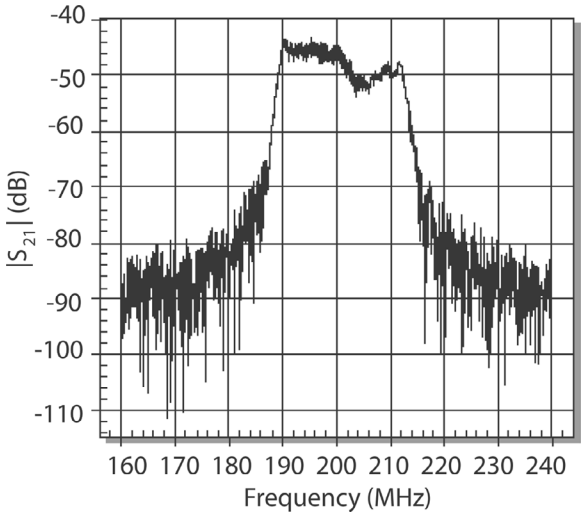

Fig. 10. Frequency response of inline DDL.

The early excellent papers of Chen and Haus [9] and Cambiaggio and Cuozzo [10] provide some fragmentary theoretical and experimental data on the reflectivity of electrodes on YZ-$LiNbO_3$. And they show that the reflectivity of open-circuited electrodes is smoothly—almost linearly—dependent on the metal ratio, which is very convenient for the control of reflectivity. The Chen and Haus

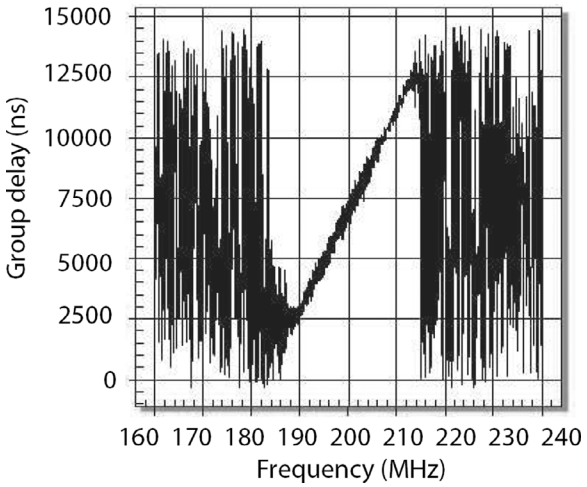

Fig. 11. Group delay of inline DDL.

data [9], calculated using a variational principle, is shown in Fig. 9 together with the simulated and experimental results of the present work.

An attempt to use narrow reflectors in inline DDLs was reported in [11]. The device geometry was similar to the type 2 devices studied above: two pairs of "mutually blind" standard IDTs were used to obtain a dispersive signal response and to suppress the direct propagation signal. The device parameters were $T = 10$ μs, $B = 24$ MHz, and $f_c = 200$ MHz. The time-gated frequency response is shown in Fig. 10. The corresponding group delay in Fig. 11. The phase deviation from quadratic was $\pm 25°$.

IV. Conclusions

A controllable reflectivity of $r < 0.3\%$ per electrode is required in order to design inline DDLs with reasonable parameters. In this work, we have demonstrated using simulations and experiments that narrow, open-circuited aluminum electrodes are perfectly suitable for this application. Reflectivities of desired magnitude can easily be achieved and controlled by varying the electrode width.

Acknowledgments

S. Härmä thanks the Jenny and Antti Wihuri Foundation, the Foundation of Technology (Finland), and the Nokia Foundation for postgraduate scholarships.

References

[1] R. Williamson and H. Smith, "The use of surface-elastic-wave reflection gratings in large time-bandwidth pulse-compression filters," *IEEE Trans. Sonics Ultrason.*, vol. SU-20, pp. 113–123, Apr. 1973.

[2] J. Gong, Y. Zhang, X. Zhou, and P. Hartogh, "Wide bandwidth SAW chirp filter with improved magnitude response," in *Proc. IEEE Ultrason. Symp.*, 2006, pp. 1895–1898.

[3] F. Huang, "Correction factor for low-loss 180° reflecting linear chirp arrays in SAW devices," *IEEE Trans. Ultrason., Ferroelect., Freq. Contr.*, vol. 35, pp. 61–65, Jan. 1988.

[4] S. Balashov, E. Garova, and V. Plessky, "Theory of Rayleigh-wave Bragg reflection in quasiperiodic structures," *Phys. Rev. B*, vol. 42, pp. 11008–11016, Dec. 1990.

[5] S. Lehtonen, V. Plessky, and M. Salomaa, "Short reflectors operating at the fundamental and second harmonics on 128° $LiNbO_3$," *IEEE Trans. Ultrason., Ferroelect., Freq. Contr.*, vol. 51, pp. 343–351, Mar. 2004.

[6] W. Wang, T. Han, X. Zhang, H. Wu, and Y. Shui, "Rayleigh wave reflection and scattering calculation for short reflector by sources regeneration method," in *Proc. IEEE Ultrason. Symp.*, 2005, pp. 459–462.

[7] C. Hartmann and R. Hartmann, "Software for multi-port RF network analysis with a large number of frequency samples and application to 5-port SAW device measurement," in *Proc. IEEE Ultrason. Symp.*, 1990, pp. 117–122.

[8] S. Lehtonen, V. Plessky, C. Hartmann, and M. Salomaa, "Extraction of the SAW attenuation parameter in periodic reflecting gratings," *IEEE Trans. Ultrason., Ferroelect., Freq. Contr.*, vol. 52, pp. 111–119, Jan. 2005.

[9] D. Chen and H. Haus, "Analysis of metal-strip SAW gratings and transducers," *IEEE Trans. Sonics Ultrason.*, vol. SU-32, pp. 395–408, May 1985.

[10] E. Cambiaggio and F. Cuozzo, "SAW reflection from conducting strips on $LiNbO_3$," *IEEE Trans. Sonics Ultrason.*, vol. SU-26, pp. 340–344, Sep. 1979.

[11] S. Balashov, V. Plessky, C. Kim, C. Nam, and V. Grigorievsky, "Dispersive delay lines based on the use of narrow open metal reflectors and fan transducer," in *Proc. IEEE Ultrason. Symp.*, 2005, pp. 2166–2169.